Evaluation of the Near-Bed Velocity Decay Resulting from a Confined Bow Thruster Jet Using PIV Measurements

Nogueira, Helena I.S.; Van Nieuwenhuizen, Christian; Bakker, Wout; Van Der Hout, Arne; Di Pietro, Paolo; Van Der Vorm, Charlotte

DOI
10.1061/JHEND8.HYENG-14383

Publication date
2026

Document Version
Final published version

Published in
Journal of Hydraulic Engineering

Citation (APA)
Nogueira, H. I. S., Van Nieuwenhuizen, C., Bakker, W., Van Der Hout, A., Di Pietro, P., & Van Der Vorm, C. (2026). Evaluation of the Near-Bed Velocity Decay Resulting from a Confined Bow Thruster Jet Using PIV Measurements. *Journal of Hydraulic Engineering*, *152*(1), Article 04025053. https://doi.org/10.1061/JHEND8.HYENG-14383

Evaluation of the Near-Bed Velocity Decay Resulting from a Confined Bow Thruster Jet Using PIV Measurements

Helena I. S. Nogueira, Ph.D.[1]; Christian van Nieuwenhuizen[2]; Wout Bakker[3]; Arne van der Hout[4]; Paolo Di Pietro[5]; and Charlotte van der Vorm[6]

Abstract: Observations in the field suggest that the existing guidelines for bed protection design may lead to overly conservative protections at berthing structures of inland vessels. In this study, physical scale model tests have been performed using particle image velocimetry to assess the near-bed velocity and the velocity decay of jets generated by transverse bow thrusters. The effect of the bed roughness, under-keel clearance (UKC) and quay wall clearance on the resulting near-bed velocities are discussed here. The results show that the maximum near-bed velocity occurs in the vicinity of the quay wall and results from an interplay between jet diffusion and the blockage effect of the nearby boundaries (e.g., quay wall, bed, and vessel), where the roughness of the confining boundary plays a role. The existing design guidelines predict fairly well the maximum near-bed velocity for smooth beds and for relatively large UKC's. However, the guidelines tend to overestimate the maximum near-bed velocities for rough beds and for small UKC's. This study proposes a new method based on measurement data to estimate the maximum near-bed velocity for confined bow thruster jets. **DOI: 10.1061/JHEND8.HYENG-14383.**

Practical Applications: This study provides new insights into how bow thruster jets affect the bed near quay walls, based on detailed physical scale model tests. The research focused on how bed roughness, under-keel clearance, and quay wall clearance influence the strength and spread of flow near the bed. Results show that rougher beds reduce flow velocities and help dissipate energy more quickly, while smaller clearances lead to stronger jets and higher velocities near the bed—conditions that can increase the risk of erosion. The findings were compared with existing design guidelines, revealing that some methods may be overly conservative, while others may underestimate flow velocities in certain areas. Based on the measurements, a new approach is proposed to better estimate near-bed velocity decay for inland vessels with bow thrusters. This can help engineers design more efficient and targeted bed protection systems. Importantly, the study was conducted under controlled, still-water conditions and focused on one type of bow thruster. Environmental factors like currents and waves were not included, so site-specific assessments remain essential. Practitioners are encouraged to use these findings alongside established guidelines to improve the safety and durability of bed protection designs.

Introduction

Over the years, inland navigation has undergone significant changes, affecting various aspects such as vessel types, sizes, propulsion systems, and thrusters. Larger vessels enable more efficient transport, but they also present challenges related to existing infrastructure, including locks, bridges, and berths. As vessels increase in size, their larger propellers, or thrusters, generate more powerful jets during maneuvering, which may exert greater hydrodynamic loads on both the quay wall and the bed beneath the vessel. In fact, most failure mechanisms of berthing structures are related to scour induced by jets of main propulsion systems and/or bow and stern thrusters (PIANC 2015). To mitigate excessive scour, some form of bed protection is typically used. In the Netherlands, there is an active focus on upgrading berthing infrastructure and promoting sustainable practices for inland navigation. In this context, the design of bed protection is identified as an area with potential for improvement.

Field studies where existing bed protections have been inspected have revealed minimal to no damage (Cantoni 2020; van der Wart 2022). Additionally, field measurements of flow velocities induced by ship jets were often lower than predicted by existing guidelines, suggesting that the current guidelines for bed protection design may be overly conservative (Tukker 2021).

Most approaches used in bed protection design are based on empirical relationships derived from a limited data set of measurements

[1]Senior Adviser and Researcher, Hydraulic Engineering Unit, Deltares, Boussinesqweg 1, Delft 2629 HV, Netherlands (corresponding author). ORCID: https://orcid.org/0000-0001-9573-0150. Email: Helena.Nogueira@deltares.nl

[2]Adviser and Researcher, Hydraulic Engineering Unit, Deltares, Boussinesqweg 1, Delft 2629 HV, Netherlands. Email: Chris.vanNieuwenhuizen@deltares.nl

[3]Adviser and Researcher, Hydraulic Engineering Unit, Deltares, Boussinesqweg 1, Delft 2629 HV, Netherlands. ORCID: https://orcid.org/0000-0002-5713-251X. Email: Wout.Bakker@deltares.nl

[4]Senior Adviser and Researcher, Hydraulic Engineering Unit, Deltares, Boussinesqweg 1, Delft 2629 HV, Netherlands; Lecturer, Faculty of Civil Engineering and Geosciences, Delft Univ. of Technology, Stevinweg 1, Delft 2628 CN, Netherlands. ORCID: https://orcid.org/0000-0003-0000-3191. Email: Arne.vanderHout@deltares.nl; A.J.vanderHout@tudelft.nl

[5]Solution Innovation and Intellectual Property Manager, DT Business Unit Corporate Technical Office, Officine Maccaferri S.p.A., Via del Faggiolo, Bologna 1/12 40132, Italy. Email: p.dipietro@maccaferri.com

[6]Senior Adviser Hydraulic Engineering, Ministry of Infrastructure and Water Management, Rijkswaterstaat, Griffioenlaan 2, Utrecht 3526 LA, Netherlands. Email: charlotte.vander.vorm@rws.nl

Note. This manuscript was submitted on October 11, 2024; approved on September 4, 2025; published online on November 10, 2025. Discussion period open until April 10, 2026; separate discussions must be submitted for individual papers. This paper is part of the ***Journal of Hydraulic Engineering***, © ASCE, ISSN 0733-9429.

(PIANC 2015; BAW 2010), which may limit the range of applicability of the existing formulas. In particular, these formulas do not account for all potential scenarios encountered in the field, such as very low under-keel and wall clearances, or vessels equipped with different types of propulsion systems and thrusters. Given the challenges and costs associated with conducting full-scale field tests, laboratory tests at a smaller scale are usually performed. However, translating laboratory results to prototype conditions also presents challenges due to potential scale effects. Furthermore, the existing guideline formulations suffer from ambiguity, often leading to confusion among engineers. The convergence of these aspects highlights the need for revised and improved guidelines to better serve the maritime engineering community. To update the existing design methods for bed protection, further knowledge of the ship-induced jets phenomenon is necessary. Specifically, estimating the maximum expected near-bed velocity, understanding where it is expected to occur, and identifying the conditions under which it occurs are of major importance.

Numerous works have been dedicated to understanding ship-induced jet flow and corresponding scour. Wei et al. (2020) provide an extensive review on the state-of-the-art knowledge in this field, focusing on experimental based works. In particular, new insights into the ship-induced jet scour phenomenon have been achieved by using optical measurement techniques such as particle image velocimetry (PIV) (Wei et al. 2017, 2018; Wei and Chiew 2019). Wei et al. (2017) investigated the effect of a smooth horizontal boundary on the development of a ship-induced jet for different bed clearances. Jet wall attachment was observed when the propeller was placed sufficiently near the bed, with jet axis placed at a distance from the bed smaller than the propeller diameter. Three different flow regions have been identified near the bed (free jet region, impingement region, and wall jet region). Wei et al. (2018) focused on the flow field within a developing scour hole around an open quay wall. Their investigation focused on mean flow patterns and turbulence characteristics, specifically on how these change with varying toe clearance fields, where toe clearance is defined as the horizontal distance between the propeller and the slope toe of the quay wall. Wei and Chiew (2019) investigated the effect of a vertical quay wall on the mean and turbulent flow fields of a ship-induced jet, for different wall clearances. Three flow regions have also been identified in their research, as function of the wall clearance. The work of these researchers have also highlighted the importance of considering turbulence characteristics in addition to the mean flow velocity when identifying the regions more susceptible to scour. Additionally, significant contributions have been made in understanding the development of scour holes for confined and unconfined propeller jets (Hong et al. 2013, 2015; Wei and Chiew 2017, 2018; Coscarella et al. 2023). Niewerth et al. (2021) and Núñez-González et al. (2022) have developed a novel method to directly measure the bottom shear stress induced by ship propeller in the laboratory, for both smooth and rough bed surfaces. The results show that bottom shear stress increased with bed roughness and with propeller rotational speed, highlighting the importance of considering the bed roughness for the correct estimation of the bed shear stress. Despite ongoing research, a comprehensive understanding of how bed roughness impacts near-bed velocities resulting from a ship-induced jet is still lacking. While some bed protection measures, such as asphalt mattresses or concrete slabs, exhibit relatively smooth surfaces, the industry predominantly uses solutions with higher roughness, such as rock-based protections (Hawkswood et al. 2024; van der Wart 2022; PIANC 2015), which may become more widely used in the future due to their potential for cost reduction and environmental considerations. A combination of protection types often coexists at one location. For instance, rock penetrated with concrete is strategically applied near the quay wall, where the highest flow velocities and highest pressure fluctuations are expected to occur, whereas loose rock may be applied at larger distances from the quay wall where flow velocities are expected to significantly decrease. However, the existing guidelines do not adequately address the effects of bed roughness.

Most of the existing literature on ship-induced scour focuses on traditional propulsion systems. However, other types of maneuvering systems, such as pump jets and four-channel bow-thrusters, are increasingly being used as robust maneuvering systems on ships and vessels of all kinds. In the Netherlands, in particular, the latter is the most common system used for maneuvering large inland vessels. The different maneuvering systems may lead to different flow patterns near the bed, and therefore to different scouring capabilities. For example, systems with more downward-directed jets may shift the location and magnitude of peak velocities along the direction perpendicular to the quay wall, influencing both the velocity decay and the spatial distribution of bed loads. This variability suggests that existing design methods, such as PIANC (2015), may incorporate safety margins that implicitly account for a broad range of vessel types and thruster configurations.

To support the update of the guidelines for the design of bed protection and to address knowledge gaps related to scour caused by ship-induced jets, a joint research program was established (Deltares 2022) joining the experience of Dutch engineering and construction companies, research institutes, and governmental representatives. The initial focus of this research program centered on near-bed flow velocities induced by confined jets generated by transverse bow thrusters. To achieve this, field measurements, laboratory experiments, and numerical simulations have been performed (Tukker 2021; Haafkes 2021; Cantoni 2020). In Tukker (2021), full-scale field measurements were performed in the Port of Gent using a large inland vessel (Somtrans XXV), equipped with a four-channel bow thruster. This study explored variations in quay wall clearance, applied power, and number of active thrusters, for a fixed under-keel clearance. Flow velocities and pressures were measured by means of point gauges [acoustic doppler velocimetry (ADV) and pressure sensors] mounted on a measurement frame beneath the vessel, above a smooth asphalt mattresses bed. The ADV sensors [type Nortek Vector, see also Tukker (2021)] were positioned at a distance ranging from 0.24 m to 0.36 m above the bed. The results from the field measurements revealed significantly lower flow velocities than those predicted by methods that are presently in use to estimate near-bed velocities. It was, however, unclear the reason for the observed differences, hence a physical scale model study was initiated.

The present manuscript focuses on the physical scale model tests performed as part of the joint research program (Deltares 2022). The field measurements performed by Tukker (2021) were used as the basis for the design of the physical scale model. The primarily objective of this study is to determine the maximum near-bed velocity, defined as the local maximum velocity, near the bed, obtained from the velocity profile along the water column, and characterize the velocity decay resulting from a confined bow thruster jet using particle image velocimetry (PIV) measurements. While many parameters have been explored in this study, this manuscript specifically focuses on the effect of the bed roughness, under-keel clearance (UKC), and quay wall clearance on the resulting flow velocities near the bed. The measurement results are compared with the existing methods used for bed protection design. Additionally, based on the experimental findings, we propose a novel method to estimate the near-bed velocity decay for inland vessels (u-shaped hulls) and equipped with transverse bow thrusters. It is important to note that the findings and the proposed alternative approach presented in

this manuscript are derived exclusively from experiments involving channel-type bow thrusters. Testing of other maneuvering systems and main propulsion units were outside the scope of this study. Our study was designed to isolate the hydraulic effects of a bow thruster in controlled conditions, providing a clear baseline for understanding jet behavior. However, we fully acknowledge that in practical applications, additional environmental factors—such as tidal currents, wave-induced motion, return flows from passing vessels, and eventually groundwater inflow—can significantly influence the velocity field and associated risks. These factors may increase the likelihood of underestimating the most vulnerable location if not properly accounted for. While our proposed approach captures the general decay behavior of the jet, it does not explicitly incorporate these external influences. This is a recognized limitation, and the results presented here are valid for still-water conditions only. For robust bed protection design, it is essential to consider a comprehensive range of loading scenarios, including vessel variability (e.g., type, propulsion system, mooring position), water level fluctuations, and exceptional events (e.g., anchor drops, dredging, spud pole impacts). We recommend that practitioners refer to established design guidelines, such as BAW (2010), which provide a framework for integrating these factors into site-specific design assessments.

Guidelines

The guidelines as described in PIANC (2015) are commonly used in the industry for the design of bed protection in maritime applications. The PIANC (2015) guidelines present a distinction between the Dutch and German methods, where the Dutch method is based on research by Blaauw and van de Kaa (1978), Verheij (1983), and Blokland (1996), whereas the German method as described in PIANC (2015) and BAW (2010) is based on research by Fuehrer et al. (1981) and Schmidt (1998). In both Dutch and German methods, the maximum near-bed velocity is a function of the thruster efflux velocity, U_0, which is defined as the maximum flow velocity of the ship-induced jet. As highlighted by Wei et al. (2020), there seems to be no general consensus on the realistic location of the efflux plane for a ship-induced jet. For nonducted main propellers, it is typically taken at the section of maximum jet contraction, $0.5D_p$, where D_p is the propeller diameter. For transverse bow thrusters, the efflux plane corresponds to the channel outlet. The efflux velocity can be obtained by applying the axial momentum theory to an ideal propeller (Albertson et al. 1950), from which the following relation (PIANC 2015) can be derived:

$$U_0 = C_1 f_n n_{\max} D_p \sqrt{K_t} \tag{1}$$

where U_0 = efflux velocity (m/s); C_1 = dimensionless coefficient; f_n = percentage of maximum number of revolutions; $n_{\max}$ = maximum number of revolutions (s^{-1}); D_p = propeller diameter (m); and K_t = dimensionless thrust coefficient. In many situations, no values are available for the number of revolutions, $n_{\max}$, and/or the thrust coefficient K_t. Therefore, empirical relationships have been derived, for example Blaauw and van de Kaa (1978) presented the following equation applicable for propellers:

$$U_0 = C_2 \left(\frac{f_p P_D}{\rho_w D_p^2} \right)^{1/3} \tag{2}$$

where C_2 = dimensionless coefficient; f_p = percentage of installed engine power; P_D = maximum installed engine power (W); and ρ_w = density of water (kg/m^3).

Table 1. List of equations to determine the efflux velocity, U_0, for transverse bow thrusters

Source	Equation		Remark
PIANC (2015)	$U_0 = \xi 1.17 \left(\frac{f_t P_D}{\rho_w D_t^2} \right)^{1/3}$	(3)	$D_t = f_t D_p$ $f_t = 1.02 - 1.05$ $\xi = 0.9 - 1.0$
BAW (2010)	$U_0 \approx 1.1 \left(\frac{P_D}{\rho_w D^2} \right)^{1/3}$	(4)	D = duct diameter (m) $D \approx D_t$
RWS ROW (2018)	$U_0 = \xi 1.17 \left(\frac{P_D}{\rho_w D_0^2} \right)^{1/3}$	(5)	$\xi = 0.9$ (inland vessels) $\xi = 1.0$ (seagoing vessels) D_0 = diameter outflow opening; for rectangular channel bow thrusters (b-width, h-height), D_0 is the equivalent circular outflow opening $D_0 = 2\sqrt{\frac{bh}{\pi}}$

Table 2. Range of the parameters L_{BT}/D_t and h_t/D_t as summarized in Tukker (2021) for the applicability of the guidelines as described in PIANC (2015) and BAW (2010), and for the field measurements by Tukker (2021) and physical scale model tests of this study

Method	L_{BT}/D_t	h_t/D_t
(PIANC 2015) Dutch method	3.2, 6.2, 12	2.66–2.86
(PIANC 2015) German method	3.97, 5.44, 7.28	1.66–3.93
Field measurements Tukker (2021)	2.89–7.99	3.03
Scale model	2.0, 3.7, 5.3	0.93, 1.70, 2.47

For transverse bow thrusters, the different guidelines (PIANC 2015; BAW 2010; RWS 2018) provide slightly different expressions for the efflux velocity, as summarized in Table 1. These differences are reflected in the value adopted for the coefficient C_2 and the considered reference diameter (duct, propeller, or outflow opening). Depending on the specific geometry of the vessel, these variations will lead to different estimations of U_0. Please note that the ξ values mentioned in Table 1 have been deliberately set conservatively in the design guidelines. Meijer and Verhey (1993) estimate ξ value for the considered type of bow thruster to be in the range 0.71–0.91. Based on personal communication with manufacturers of this type of bow thruster systems, a value around $\xi = 0.75$ is deemed realistic. The ambiguity in the definition of U_0 makes it unclear which expression and parameters should be used. In the present research, U_0 is determined experimentally and used as a velocity scale for normalization. However, a correct definition of U_0 remains important for design.

Table 2 presents an overview of the parameters and respective ranges used in the existing methods to estimate velocities, namely the quay wall clearance L_{BT}, normalized by the thruster diameter D_t, and the height of the bow thruster axis above the bed h_t, also normalized by the thruster diameter. The parameter D_t serves as the normalization factor, consistent with prior studies (Tukker 2021). Please refer to Fig. 1 for the meaning of the parameters. In Table 2 is also included the field measurements from Tukker (2021) and physical scale model tests for comparison. The values in the table for the PIANC (2015) guidelines are based on research by Blokland (1996) for the Dutch method, and by Fuehrer et al. (1981) and Schmidt (1998) for the German method, as cited in Tukker (2021).

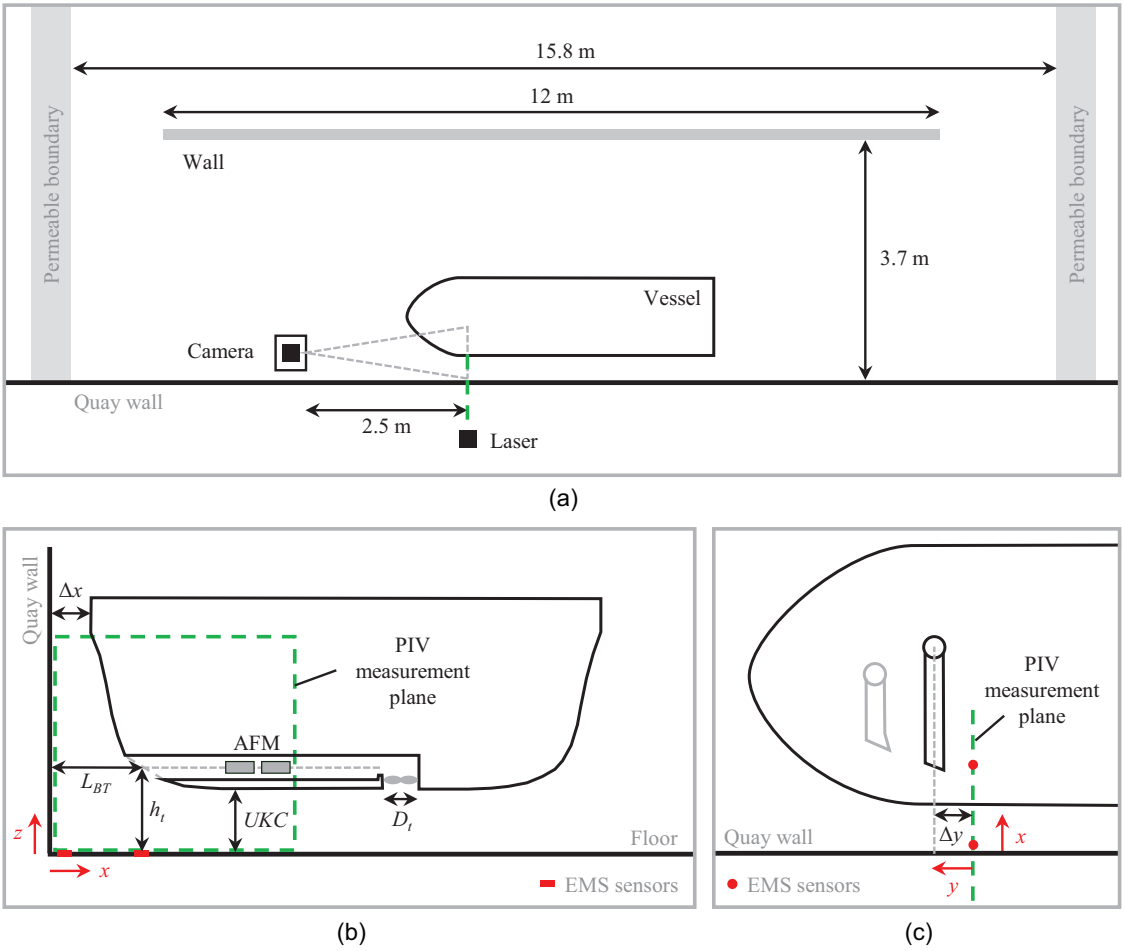

Fig. 1. (Color) Schematization of the test setup and the main parameters: (a) top view of the test setup, distances in model scale; (b) cross-section view through the centerline of the bow thruster channel; and (c) detail of the top view.

According to the existing guidelines, the maximum flow velocity near the bed occurs at the point where it intersects with the quay wall. The equations used for estimating the maximum flow velocity at this location, $U_{b,\max}$, as provided by different methods in PIANC (2015) and BAW (2010), are summarized in Table 3. Please note that both the guidelines in BAW (2010) and the Dutch method in PIANC (2015) use the same equations for estimating the maximum flow velocity near the bed [Eqs. (6), (7), (11), and (12)].

Table 4 presents the formulations used to estimate the decay in the x-direction of the maximum near-bed velocity, $U_{b,\max}(x)$. Please note that the German method does not provide a method to account for the velocity decay of the reflected jet. In the equations presented in Tables 3 and 4, the Dutch method and BAW (2010) estimate the total horizontal velocity near the bed [combining u and v components, Eqs. (6), (7), (11) and (12)], whereas the German method provides an estimation for the u-component only [Eqs. (8)–(10)].

Table 3. List of equations for the maximum near-bed velocity for transverse thrusters

Source	Equation		Remark
(PIANC 2015) Dutch method	$\frac{U_{b,\max}}{U_0} = \frac{D_t}{h_t}$	(6)	$\frac{L_{BT}}{h_t} < 1.8$
	$\frac{U_{b,\max}}{U_0} = 2.8\left(\frac{D_t}{L_{BT}+h_t}\right)$	(7)	$\frac{L_{BT}}{h_t} \geq 1.8$
(PIANC 2015) German method	$U_{wall} = U_0$	(8)	$\frac{L_{BT}}{D_t} < 1.9$
	$U_{wall} = 1.9U_0\left(\frac{D_t}{L_{BT}}\right)$	(9)	$\frac{L_{BT}}{D_t} > 1.9$
	$\frac{U_{b,\max}}{U_{wall}} = 10.6\left(\frac{D_t}{L_{BT}}\right)\left(\frac{h_t}{Dt}\right)^{-1.15}$	(10)	
BAW (2010)	$\frac{U_{b,\max}}{U_0} = \frac{D_t}{h_t}$	(11)	$\frac{L_{BT}}{h_t} < 1.8$
	$\frac{U_{b,\max}}{U_0} = 2.8\left(\frac{D_t}{L_{BT}+h_t}\right)$	(12)	$\frac{L_{BT}}{h_t} \geq 1.8$

Table 4. List of equations for the decay of the maximum near-bed velocity for transverse thrusters

Source	Equation		Remark
(PIANC 2015) Dutch method	$\frac{U_{b,\max}}{U_0} = \frac{D_t}{h_t}$	(13)	$\frac{L_{BT}+x}{h_t} < 1.8$
	$\frac{U_{b,\max}(x)}{U_0} = 2.8\left(\frac{D_t}{L_{BT}+h_t+x}\right)$	(14)	$\frac{L_{BT}+x}{h_t} \geq 1.8$
BAW (2010)	$\frac{U_{b,\max}(x)}{U_0} = \frac{D_t}{h_t}\left(\frac{L_{BT}+h_t}{L_{BT}+h_t+x}\right)^{1.62}$	(15)	$\frac{L_{BT}}{h_t} < 1.8$
	$\frac{U_{b,\max}(x)}{U_0} = 2.8D_t\frac{(L_{BT}+h_t)^{0.62}}{(L_{BT}+h_t+x)^{1.62}}$	(16)	$\frac{L_{BT}}{h_t} \geq 1.8$

J. Hydraul. Eng., 2026, 152(1): 04025053

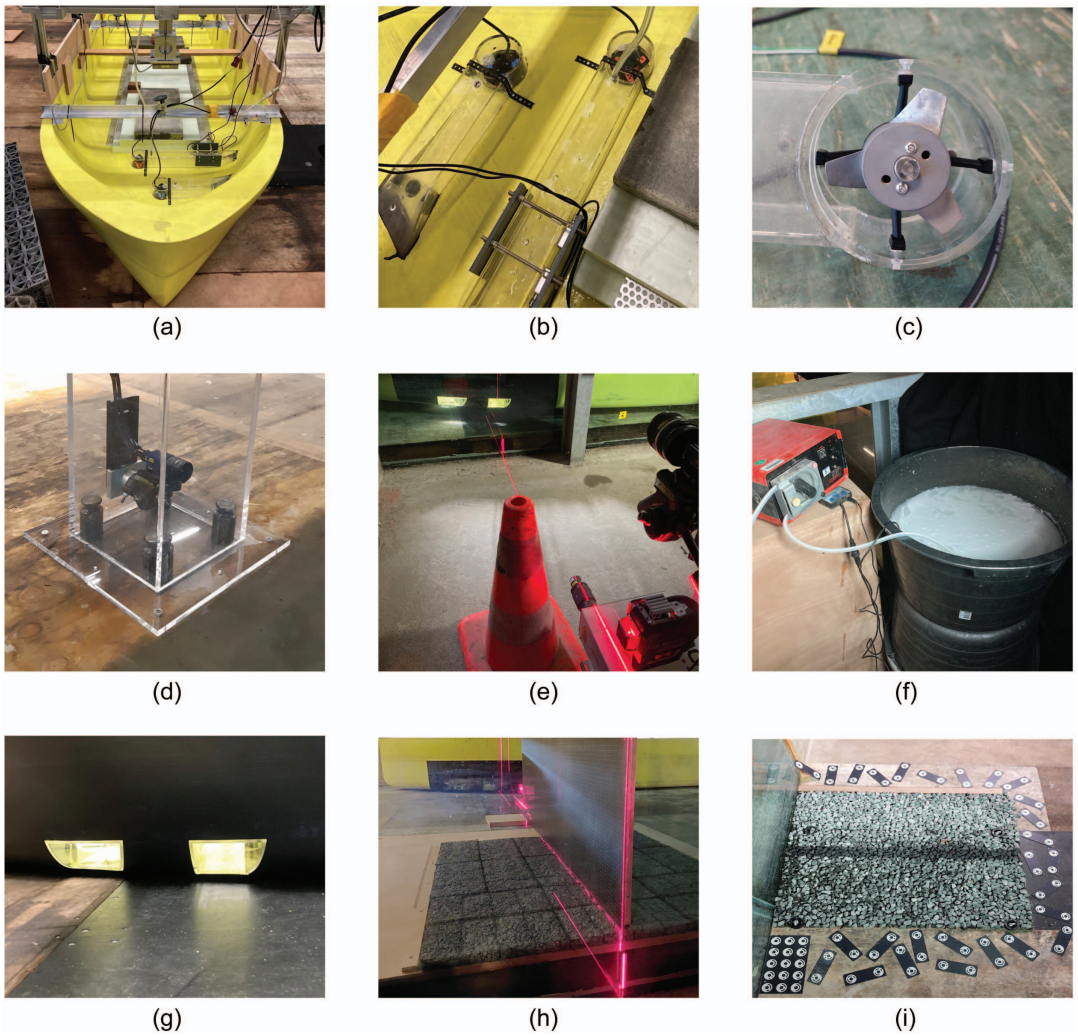

Fig. 2. (Color) Photographs of the experimental setup.

Description Scale Model

The scale model tests were designed with a scale factor of 1:14.44, based on the ratio of prototype to model thruster inlet diameter. Scaling is based on the Froude scaling principle where the ratio between gravitational and inertial forces is kept constant between the scales. Fig. 2 provides an overview of the scale model and experimental setup. The scale model consists of a model vessel [replica of the Somtrans XXV, Tukker (2021)], featuring a u-shaped hull with a beam of 17.5 m and a length of 135 m (prototype scale values), as shown in Fig. 2(a). In the scale model only half of the vessel length was considered as the primary region of interest is the surroundings of the bow. The model vessel was supported by an aluminum frame via which the vessel can be positioned at different locations relative to the quay wall. The quay wall itself is represented by a clear and smooth glass wall such that there is the required optical access for the PIV measurements. However, this deviates from the actual field conditions, where the quay wall consists of a sheet pile structure, introducing inherent roughness to the wall surface. The effect of the quay wall roughness on the jet reflection at the wall is not considered in the present research, however it should be further investigated. The vessel has two bow thrusters, however only the rearmost thruster was used for the purpose of this study [see test setup in Figs. 1 and 2(b)]. The model propeller and thruster inlet is shown in Fig. 2(c). The PIV measurements produce velocity fields in a plane perpendicular to the vessel and quay wall, in a plane through the centerline of the bow thruster channel, or in planes parallel to the jet centerline (see Fig. 1).

The PIV system consists of a LaVision Imager MX4M camera (10 bit dynamic range, equipped with a 35 mm lens, $f^{\#} = 5.6$ [-]), a double-pulsed laser (Litron Nano L 50-100 PIV, output energy 50 mJ/pulse, light wavelength 532 nm and pulse duration 8 ns), controlled by DaVis software (8.4.0). The PIV camera, mounted in a watertight transparent box in the test basin [see Fig. 2(d)], is positioned 2.5 m from the laser sheet (measurement plane thickness approximately 4 mm), resulting in a PIV measurement region of approximately 55×55 cm^2. Fig. 2(e) illustrates the location of the laser head and the laser alignment procedure. The flow is seeded with 100-micron polyamide particles (Vestosint 1101, $\rho_p = 1060$ kg/m^3), injected directly into the bow channel [see Fig. 2(f)]. The time between the laser pulses varies with the flow velocity of the measurement condition such that the interframe displacement is kept relatively constant (i.e., high flow velocities correspond to shorter interframe times, while longer interframe times are set for low flow velocity conditions). Each image is subdivided in interrogation windows of 32×32 pixels, with a 50% overlap, resulting in a vector spacing of 4.3 mm/vector. The PIV measurement conditions are set to meet all four PIV design rules, i.e., sufficient particle density, limited in- and out-of-plane loss of particles and limited local

spatial velocity gradients, as outlined by Adrian and Westerweel (2011). This ensures results with over 95% valid vectors within the instantaneous velocity fields, and an overall PIV-measurement error of the velocity in the order of 1%, corresponding to 0.1 pixel error of the interframe displacement in each interrogation window, which is introduced as a rough estimate of the PIV uncertainty (Adrian and Westerweel 2011). For postprocessing of the instantaneous velocity fields, a universal outlier detection (Westerweel and Scarano 2005) is applied to detect spurious vectors, which are replaced by velocity vectors corresponding to alternative correlation peaks. For all PIV tests, 1,000 instantaneous velocity fields are obtained, each based on the spatial cross correlation of the images of a frame pair. The acquisition rate of frame pairs is set to 2 Hz, ensuring time-independent samples of the velocity field. The velocity fields here presented are the time-averaged values at each vector location of the total time-series of a PIV test. The number of frame pairs (1,000) was found to be sufficient for the statistics as presented in this work to reach convergence.

Two nonintrusive electromagnetic flow meters (EMS, Deltares EMS E40-Flush-A, with an accuracy of 1 cm/s ± 1% of the measured velocity) were flush mounted on the set-up floor along the jet centerline. Each EMS measures horizontal velocity vectors (u and v velocity components) at the two locations depicted in Fig. 1 at approximately 5 mm above the floor. These sensors were exclusively applied during tests with a smooth bed. An acoustic flow meter (AFM, KATflow 150, with a measurement accuracy of 0.5% of the measured velocity) was installed in the outer walls of the bow thruster channel to measure the flow velocity (U_{BT}), which was used to quantify the jet efflux velocity U_0 during testing [see Fig. 2(b)]. Both the velocity signal of the EMS's and the AFM are sampled at a rate of 120 Hz with a digital acquisition system. The velocity values of the EMS's and AFM as presented are all based on the time-average value of the acquired time series.

Tests

This study investigates the effect of many parameters, such as UKC, propeller power, bed roughness, quay wall clearance, number of active thrusters and PIV measurement plane, leading to a large number of experiments where over 100 different PIV tests have been performed. A selection of 18 PIV tests is presented in Table 5 where the quay wall clearance (L_{BT}), PIV measurement plane (Δy), UKC and bed roughness have been varied. The height of the axis of the bow thruster channel above the bed is given by $h_t = \text{UKC} + 0.715$ m. Please note that all values are here presented in prototype scale. This is to ensure direct applicability and alignment with professional practice, and to reflect the collaborative nature of the study with engineering firms and facilitating immediate interpretation within real-world operational contexts.

For normalization, the efflux velocity U_0 is used as the velocity scale, while the inlet diameter of the bow thruster channel ($D_t = 1.3$ m), is used as a length scale, in alignment with previous studies. The efflux velocity was derived from the experiments by measuring the flow velocity in the bow thruster channel, U_{BT}. The relationship between U_{BT} and U_0 was derived from dedicated tests, where a combination of PIV measurements and AFM measurements on an unconfined (free) bow thruster jet was performed, resulting in $U_0 \approx 1.1 U_{BT}$, where U_{BT} is the area averaged outflow velocity (based on the AFM measurements) and U_0 corresponds to the maximum measured outflow velocity (based on the PIV measurements). Noting that the measurement uncertainties of the AFM and PIV measurements are approximately 0.5% and 1% respectively, the ratio between U_0 and U_{BT} of 1.1 is obtained with a relative error of 1.5%.

The UKC was varied by adapting the water level in the basin and the quay wall clearance was changed by shifting the vessel perpendicular to the quay wall. Although the lowest tested UKC (0.5 m, with a corresponding ratio $h_t/D_t = 0.93$) is not realistic for typical conditions, it was decided to test this condition to gain insight into the flow behavior at such exceptionally low UKC.

The influence of the bed roughness was tested by changing the bed material leading to smooth and rough (nonerodible) bed tests. A smooth bed was represented in the model by a wooden floor [see Fig. 2(g)], whereas rock-based protections were used to create bed roughness. The rock-based protections considered were fixed rock [see Fig. 2(i)] and a special type of prefilled rock mattress [see Fig. 2(h)], specifically designed for underwater applications (Deltares 2023; van Nieuwenhuizen et al. 2024; Brocca et al. 2024). For the fixed rock, a grading 10–60 kg was selected where rock was glued to the wooden floor. For the prefilled rock mattress, rocks with grading 100–130 mm were used. These were encased in a double twisted steel wire mesh unit with uniformly partitioned double pleated

Table 5. Test overview with main varied parameters

Test	L_{BT} (m)	Δx (m)	Δy (m)	UKC (m)	U_{BT} (m/s)	L_{BT}/D_t	ht/D_t	Roughness	Bed material
1	2.63	0.8	0.0	2.5	4.4	2.03	2.47	Smooth	Flat wooden plate
2	2.63	0.8	0.0	1.5	4.6	2.03	1.70	Smooth	Flat wooden plate
3	2.63	0.8	0.0	0.5	4.6	2.03	0.93	Smooth	Flat wooden plate
4	2.63	0.8	0.0	2.5	4.8	2.03	2.47	Intermediate	Prefilled rock mattress
5	2.63	0.8	0.0	1.5	4.6	2.03	1.70	Intermediate	Prefilled rock mattress
6	2.63	0.8	0.0	0.5	4.7	2.03	0.93	Intermediate	Prefilled rock mattress
7	2.63	0.8	0.0	2.5	4.7	2.03	2.47	Rough	Rock 10–60 kg
8	2.63	0.8	0.0	1.5	4.6	2.03	1.70	Rough	Rock 10–60 kg
9	2.63	0.8	0.0	0.5	4.5	2.03	0.93	Rough	Rock 10–60 kg
10	4.84	3.0	0.0	2.5	5.0	3.73	2.47	Smooth	Flat wooden plate
11	6.84	5.0	0.0	2.5	5.0	5.26	2.47	Smooth	Flat wooden plate
12	4.84	3.0	0.0	2.5	4.8	3.73	2.47	Intermediate	Prefilled rock mattress
13	4.84	3.0	0.0	2.5	4.7	3.73	2.47	Rough	Rock 10–60 kg
14	2.63	0.8	−4.0	2.5	4.7	2.03	2.47	Smooth	Flat wooden plate
15	2.63	0.8	−2.0	2.5	4.8	2.03	2.47	Smooth	Flat wooden plate
16	2.63	0.8	2.0	2.5	4.7	2.03	2.47	Smooth	Flat wooden plate
17	2.63	0.8	3.5	2.5	4.7	2.03	2.47	Smooth	Flat wooden plate
18	4.84	3.0	0.0	0.5	4.8	3.73	0.93	Smooth	Flat wooden plate

Note: Values presented in prototype scale (scale factor 1:14.44).

J. Hydraul. Eng., 2026, 152(1): 04025053

diaphragms and vertical connections. Units were equipped with an extra layer made of wire mesh and geotextile, extended on two sides beyond the perimeter, to allow continuous protection to the adjacent units. For both the fixed rock and the rock-filled mattresses, the UKC is measured from the top surface of the rock or mattress layers.

A start-up measurement of 10 min duration (model scale) was performed to capture the start-up phase of the propeller. In this phase no PIV measurement was performed; instead, all remaining measurement signals (i.e., time-series of the AFM, EMS's, water levels, and RPM's of the motor) were acquired. Following the start-up test, while the propeller remained active, the PIV measurement started. For all performed tests, an 8-min (model scale) PIV measurement was performed, corresponding to the acquisition of 1,000 frame pairs at a 2Hz frequency. Simultaneously, velocity measurements are conducted with the two EMS's and the AFM. The same testing procedure was followed for all performed tests.

Results and Discussion

Flow Patterns

Fig. 3 presents the contour map of the normalized time-averaged flow velocity (u and w components combined) for Test 1 (see Table 5), performed for a smooth bed, UKC = 2.5 m and $\Delta x =$ 0.8 m, herein used as the reference test. This figure illustrates the main time-averaged flow patterns observed in the vertical plane at the centerline of the jet. A distinction is made here between the main jet, i.e., the jet exiting the bow thruster channel where the highest flow velocities are measured, and the reflected jet, which refers to the jet directed toward the bed. The main jet spreads in all directions upon reaching the vertical wall. The upward and downward flows in the vicinity of the wall are captured in Fig. 3, as well as the confined recirculating cell above the main jet, situated between the vessel and the wall, and the broader recirculation flow pattern underneath the vessel. The decay of the maximum time-averaged near-bed velocity, $U_{b,\max}(x)$, is determined based on the PIV measurements by taking the maximum value of the time-averaged

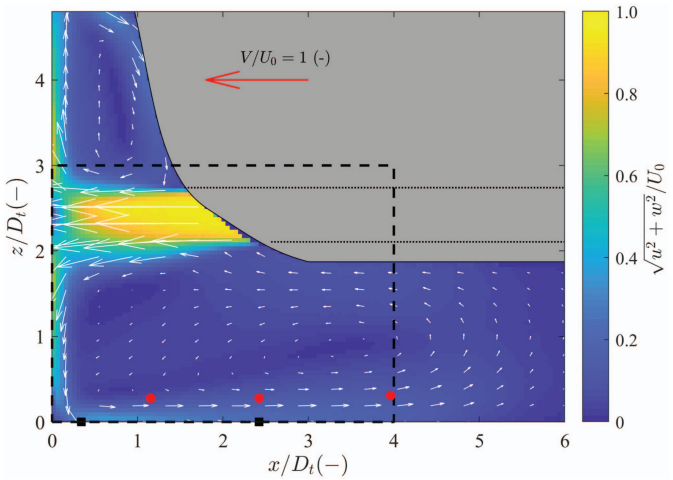

Fig. 3. (Color) Time-averaged velocity magnitude (u and w components) for Test 1. Dashed rectangle illustrates the area measured in the selected tests. Squares represent the location of the two EMS sensors used to measure locally the u and v near-bed velocity components. Circles represent the ADV measurement locations in the field measurements by Tukker (2021).

u-velocity component within one meter from the bed (0 m < z < 1 m, or $0 < z/D_t < 0.7$), at each x measured location. Near the bed, the vertical velocity component w is negligible in comparison with the u component, therefore only the u component is here presented for discussion. Point gauges (electromagnetic sensors, represented by black squares in Fig. 3) were used in selected tests performed with a smooth bed to measure locally u and v velocity components to verify the u-component measured with PIV and to get an estimate of the v-component. The dashed rectangle in Fig. 3 presents the flow area focused in Fig. 4. Also in Fig. 3 is represented by red circles the location of the measurement region captured by the ADV sensors in the field measurements by Tukker (2021). Although careful comparison between scale model data and field measurements should be made due to potential scale effects, this figure illustrates a possible cause for lower than expected velocities observed in the field measurements. It shows that the location of the ADV sensors may not have been ideal to capture the maximum flow velocities near the bed, especially closer to the quay wall (two first sensors), as the sensors could have been capturing the core of the recirculating flow pattern created by the interaction between the main jet and the reflected jet near the bed.

Fig. 4 illustrates the measured flow patterns for the variation of two parameters: UKC (constant value per row) and bed roughness (constant roughness per column). This figure shows that, over a smooth bed, the reflected jet spreads in a seemingly horizontal way toward the vessel provided that there is sufficient space underneath the vessel for the jet to propagate [Figs. 4(a and d)]. As the bed roughness increases, the reflected jet gradually moves upward, detaching from the bed [e.g., Figs. 4(b and c), or (e and f)]. Part of the upward flow is incorporated by the main jet, creating a localized recirculating cell in the vertical plane underneath the vessel. The higher the bed roughness, the closer to the quay wall flow detachment occurs. As the UKC is reduced, the propagation of the reflected jet near the bed starts to be influenced by the main jet and by the blockage of the vessel. The most obvious effect is the recirculating flow underneath the vessel becoming more confined and closer to the quay wall, which is expected to increase the near-bed velocity due to less space available for the jet to dissipate [Figs. 4(g–i)].

Fig. 5 illustrates the measured flow patterns for a variation in quay wall clearance. The more space available there is between vessel and quay wall, more jet spreading and momentum decrease will occur before the main jet reaches the quay wall, consequently lower velocities will impact the bed. At a distance of $\Delta x = 5$ m from the quay wall ($L_{BT}/D_t = 5.26$), the wall still has an effect on the jet propagation, highlighted by the return flow above and below the main jet outflow [Fig. 5(c)].

Maximum Near-Bed Velocity and Velocity Decay

Effect of Bed Roughness and UKC

Fig. 6 presents the decay of the maximum time-averaged near-bed velocity for the combination of tests presented in Fig. 4. These tests involve the smallest distance between vessel and the quay wall ($\Delta x = 0.8$ m, $L_{BT}/D_t = 2.03$), for a varying UKC and bed roughness. The plotted lines represent the u-component measured with PIV (with an uncertainty of approximately 1% of the measured velocity), and the u and v velocity components measured with point gauges (EMS, with an uncertainty of 1% of the measured velocity) are also presented for comparison (smooth bed only). In addition, the maximum near-bed velocity as predicted by PIANC (2015) and BAW (2010) guidelines are also presented. This figure shows that:

- The measured near-bed velocity is nearly zero (stagnation point) at the intersection with the quay wall, which contradicts the predictions of existing guidelines.

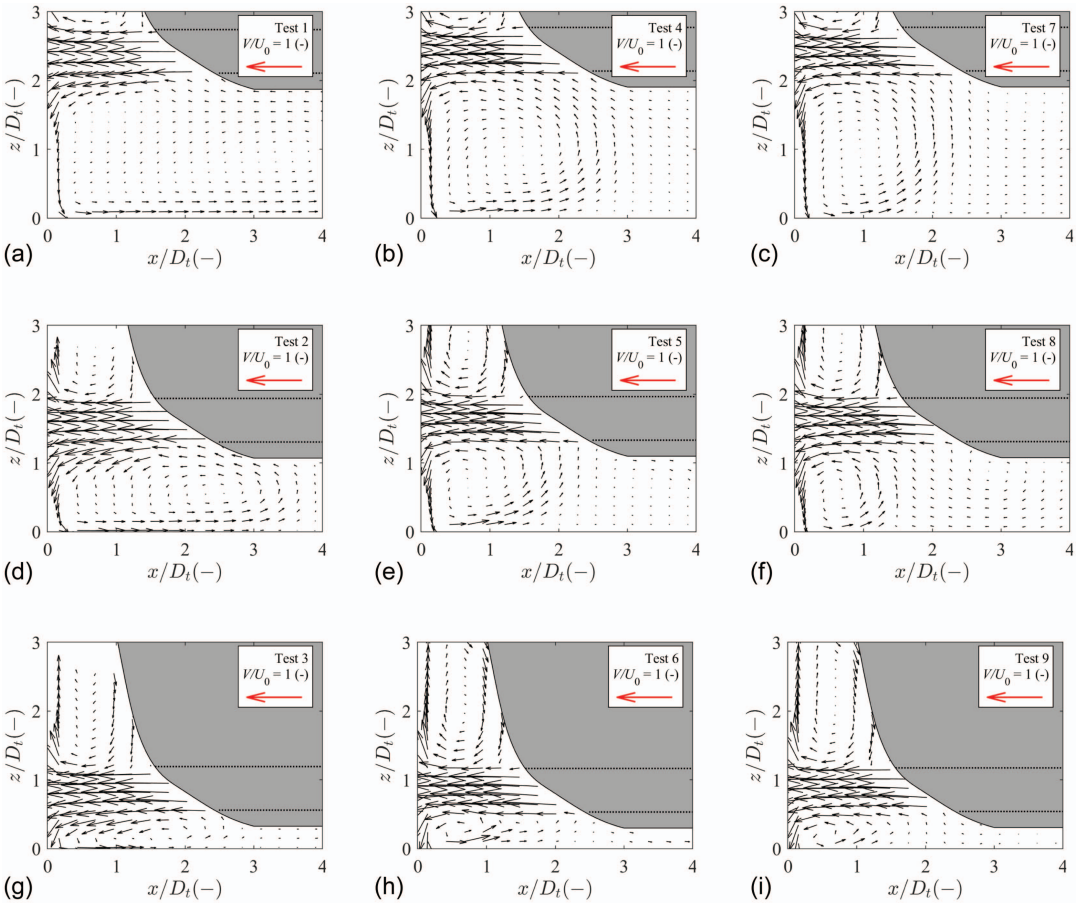

Fig. 4. (Color) Time-averaged vector fields (u and w components) measured with PIV in the centerline of the jet ($\Delta y = 0$ m), for $\Delta x = 0.8$ m ($L_{BT}/D_t = 2.03$) for different under-keel clearances and different bed roughness: (a) test 1; (b) test 4; (c) test 7; (d) test 2; (e) test 5; (f) test 8; (g) test 3; (h) test 6; and (i) test 9.

- The near-bed velocity increases rapidly with the distance from the quay-wall, typically reaching a peak at a distance roughly within $x/D_t < 1$; the rate of velocity increase is consistent across tests just before reaching this peak.
- After the maximum velocity, the near-bed velocity gradually decreases. The rate of decay varies between tests, influenced by the interplay between bed roughness and available clearance between vessel, quay wall, and floor. Bed roughness tends to reduce the maximum flow velocity and leads to a sharper velocity decay.
- Generally, there is good agreement between the PIV measurements and the point measurements (specifically the u-component) at the two measured locations (for a smooth bed). However, PIV measurements tend to underestimate the highest velocity measured (Adrian and Westerweel 2011). This discrepancy may be due to suboptimal measurement conditions near the bed where velocities are highest.
- Smaller UKC results in increased velocity magnitude. Regarding the flow direction, the return flow near the bed will gradually spread more in the direction along the quay wall (y-direction) as UKC is reduced. Very close to the quay wall, the flow is predominantly directed toward the vessel, as indicated by the dominance of the u velocity component.

Regarding the comparison with the guidelines:

- The maximum velocity estimated by the Dutch method in PIANC (2015) and the guidelines from BAW (2010) generally match well with the PIV measurements. However, for the smallest UKC tested (0.5 m), all existing methods overestimate the maximum velocity and velocity decay.
- The German method in PIANC (2015) overestimates the maximum velocity for the small quay wall clearance tested ($\Delta x = 0.8$ m, $L_{BT}/D_t = 2.03$) and is insensitive to changes in UKC for this small wall clearance. This is because the German formulation is only applicable for larger wall clearances ($L_{BT}/D_t > 3.97$, see Table 2).
- Both the German and Dutch methods in PIANC (2015) and BAW (2010) identify the location of the maximum velocity at the intersection with the quay wall. In the scale model, the maximum velocity was measured at a distance from the wall roughly within $x/D_t < 1$.
- The guidelines from BAW (2010) generally provide a more reasonable estimation for the trend of velocity decay, showing good agreement with the measurements for a smooth bed. However, it underestimates the maximum velocity, particularly for smooth bed cases [see Figs. 6(a and b)]. This underestimation may result in a potential risk of bed erosion.

Note that the velocity values estimated by the different guidelines are all based on the geometric properties of the setup (i.e., D_t, L_{BT}, h_t, and x). It is assumed that these properties each have an uncertainty of 1% of their values, resulting in an estimated error of the velocities estimated by the guidelines of 2%–4%.

Fig. 7 presents the velocity decay for a fixed quay wall clearance of $\Delta x = 3.0$ m and UKC of 2.5 m ($L_{BT}/D_t = 3.73$, $h_t/D_t = 2.47$), for a varying bed roughness. Compared to the smaller wall

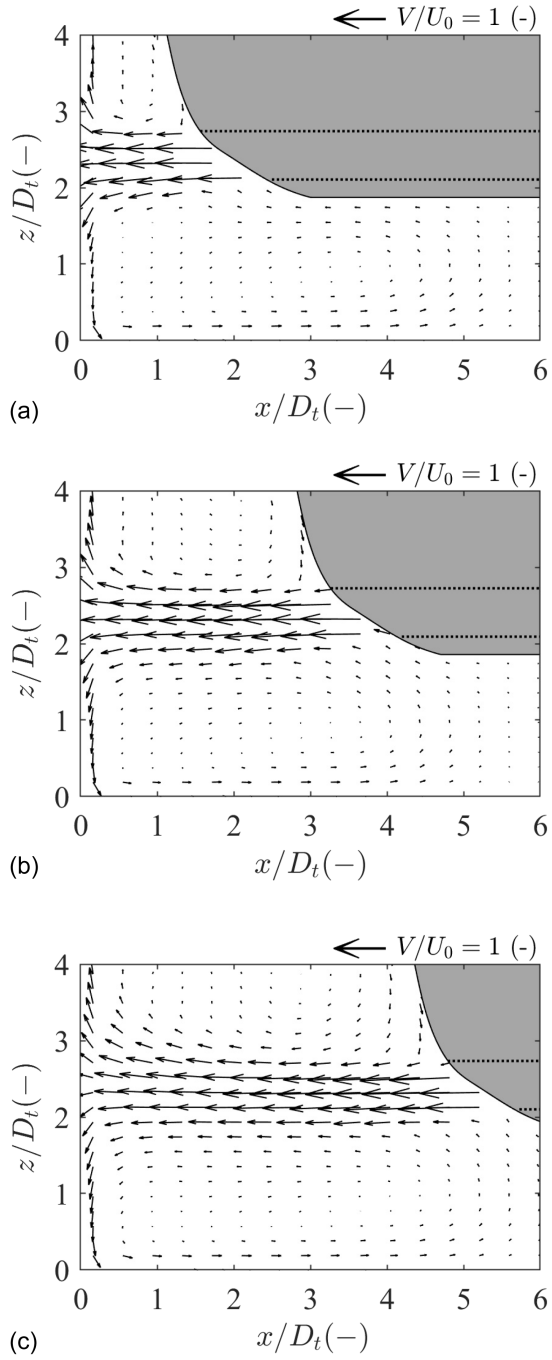

Fig. 5. Time-averaged vector fields (u and w components) measured with PIV in the centerline of the jet ($\Delta y = 0$ m), for UKC = 2.5 m ($h_t/D_t = 2.47$) for different quay wall clearances: (a) test 1; (b) test 10; and (c) test 11.

clearance ($\Delta x = 0.8$ m), the effect of the bed roughness on the maximum near-bed velocity is less pronounced. The velocity decay is less sharp, when comparing with Fig. 6(a), due to the additional space available for the jet to propagate. The velocity decay trend and its variation with roughness remain comparable to what was observed for a smaller wall clearance.

Effect of Varying Measurement Plane in the y-Direction

Fig. 8 presents the velocities measured in different planes parallel to the jet centerline, providing insights into the spatial distribution of near-bed velocities in the y-direction. This figure shows that the jet does not spread symmetrically relative to the thruster channel centerline, where most flow is directed toward the stern (negative Δy values). In particular, the maximum flow velocity near the bed is not located at the plane of the channel axis. Instead, it is slightly toward the stern of the vessel ($\Delta y = -2$ m). This behavior is likely influenced by the bow thruster channel outlet geometry (refer to Fig. 1). Fig. 8 also highlights that the BAW (2010) guidelines are not conservative in this situation, underestimating the near-bed velocities away from the wall.

Effect of Varying the Quay Wall Clearance

Fig. 9 illustrates the effect of varying the quay wall clearance on a smooth bed. The velocity decay trend is shown in Fig. 9(a) for a large UKC (2.5 m), where small differences between tests are observed. For a small UKC [0.5 m, Fig. 9(b)], the effect of the quay wall clearance becomes more pronounced. In both cases, higher velocities are measured for the smaller wall clearance. Figs. 9(c and d) illustrate the mechanisms responsible for velocity decay with a small clearance (0.5 m) seen in Fig. 9(b): for $\Delta x = 0.8$ m [Fig. 9(c)] the velocity decay near the bed (first decay trend, $0.8 < x/D_t < 1.5$) is influenced by the main jet, whereas the second decay trend ($1.5 < x/D_t < 3$) is influenced by the blockage of vessel's hull. For $\Delta x = 3.0$ m [Fig. 9(d)], the main obstacle to the propagation of the reflected jet is the influence of the main jet.

Alternative Method

Based on the existing guidelines and measurement data, we propose an alternative formulation for estimating the maximum near-bed velocity and the subsequent velocity decay. The aim is to reduce some of the conservatism in the decay trend of the maximum velocity as estimated by the Dutch method, and to better adjust to the measurement data for the tested range of parameter variation (see Fig. 10). Table 6 summarizes the equations for the maximum velocity and velocity decay for the proposed method. While this method does not explicitly include a parameter for bed roughness, it provides a conservative estimate for the maximum velocity based on all tested bed roughness conditions. In this method, the maximum velocity near the bed remains consistent with the Dutch or BAW methods for $L_{bt}/h_t < 1$, in the vicinity of the quay wall where the maximum velocity is expected to occur ($x/D_t < 1$). Beyond this point, we adopt a decay trend based on the BAW method, with slight adjustments to improve the match with the measurement data.

Overview All Tests

In Fig. 10 are summarized the results of all tests conducted in this research, considering variations in wall clearance, bed roughness, UKC, measurement plane and propeller power. This figure shows that:

- The German method in the PIANC (2015) guidelines tends to overestimate the maximum velocity for most tested conditions, except for the largest wall clearance tested ($\Delta x = 5$ m) and largest under-keel clearance (UKC = 2.5 m), illustrated in Fig. 10(c). This specific condition is the only one in the tested range that falls within the range of application of the German method, and for this condition the prediction by this method is not conservative.
- The Dutch method in the PIANC (2015) guidelines generally provides conservative estimates for the maximum near-bed velocity and velocity decay. However, there are exceptions: at $\Delta x = 0.8$ m and UKC = 1.5 m [Fig. 10(d)], slightly higher velocities were measured near the quay wall using point gauges.
- The BAW (2010) guidelines yield the same maximum velocity estimation as the Dutch method but exhibit a decay trend that aligns better with the measured data. According to this

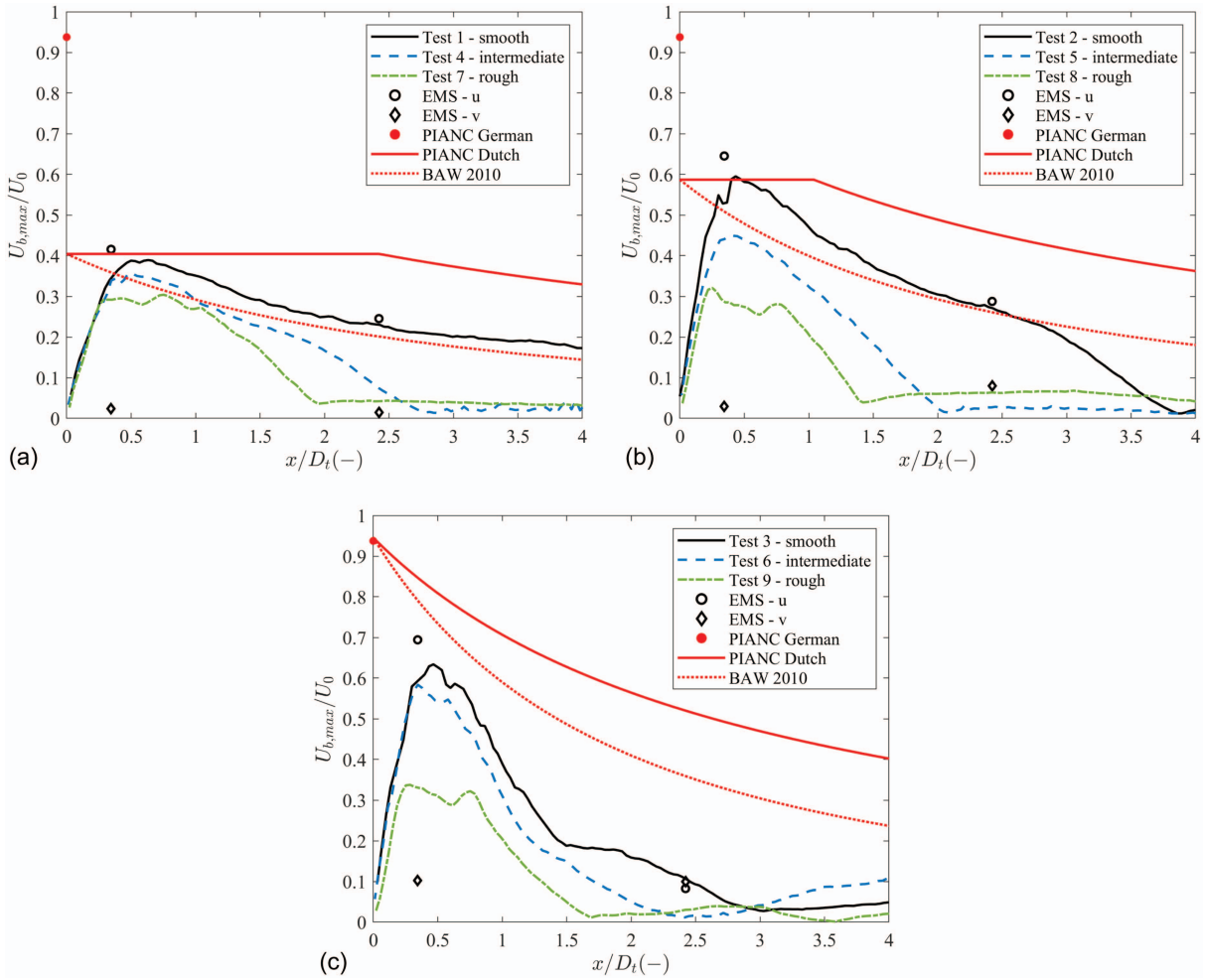

Fig. 6. (Color) Normalized decay of the maximum time-averaged velocity for $\Delta y = 0$ m and $\Delta x = 0.8$ m ($L_{BT}/D_t = 2.03$), for a varying UKC and varying bed roughness: (a) UKC = 2.5 m; (b) UKC = 1.5 m; and (c) UKC = 0.5 m.

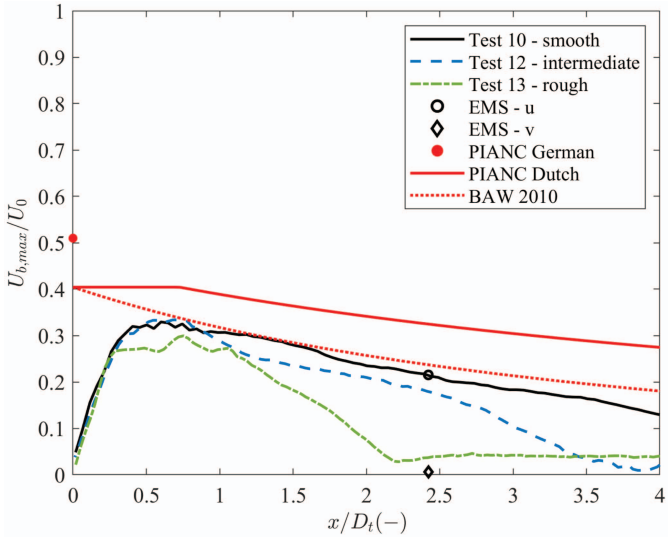

Fig. 7. (Color) Normalized decay of the maximum time-averaged near-bed velocity for UKC = 2.5 m ($h_t/D_t = 2.47$), $\Delta x = 3.0$ m ($L_{BT}/D_t = 3.73$) and $\Delta y = 0$ m, for varying roughness.

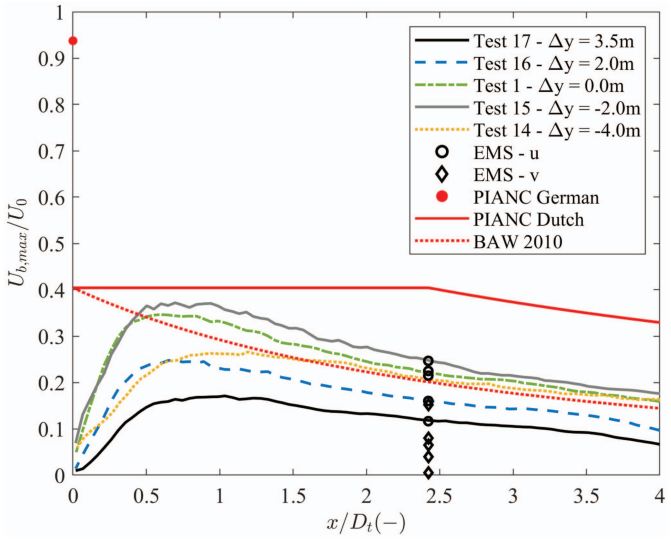

Fig. 8. (Color) Normalized decay of the maximum time-averaged near-bed velocity for UKC = 2.5 m ($h_t/D_t = 2.47$), $\Delta x = 0.8$ m ($L_{BT}/D_t = 2.03$), smooth bed and varying Δy.

J. Hydraul. Eng., 2026, 152(1): 04025053

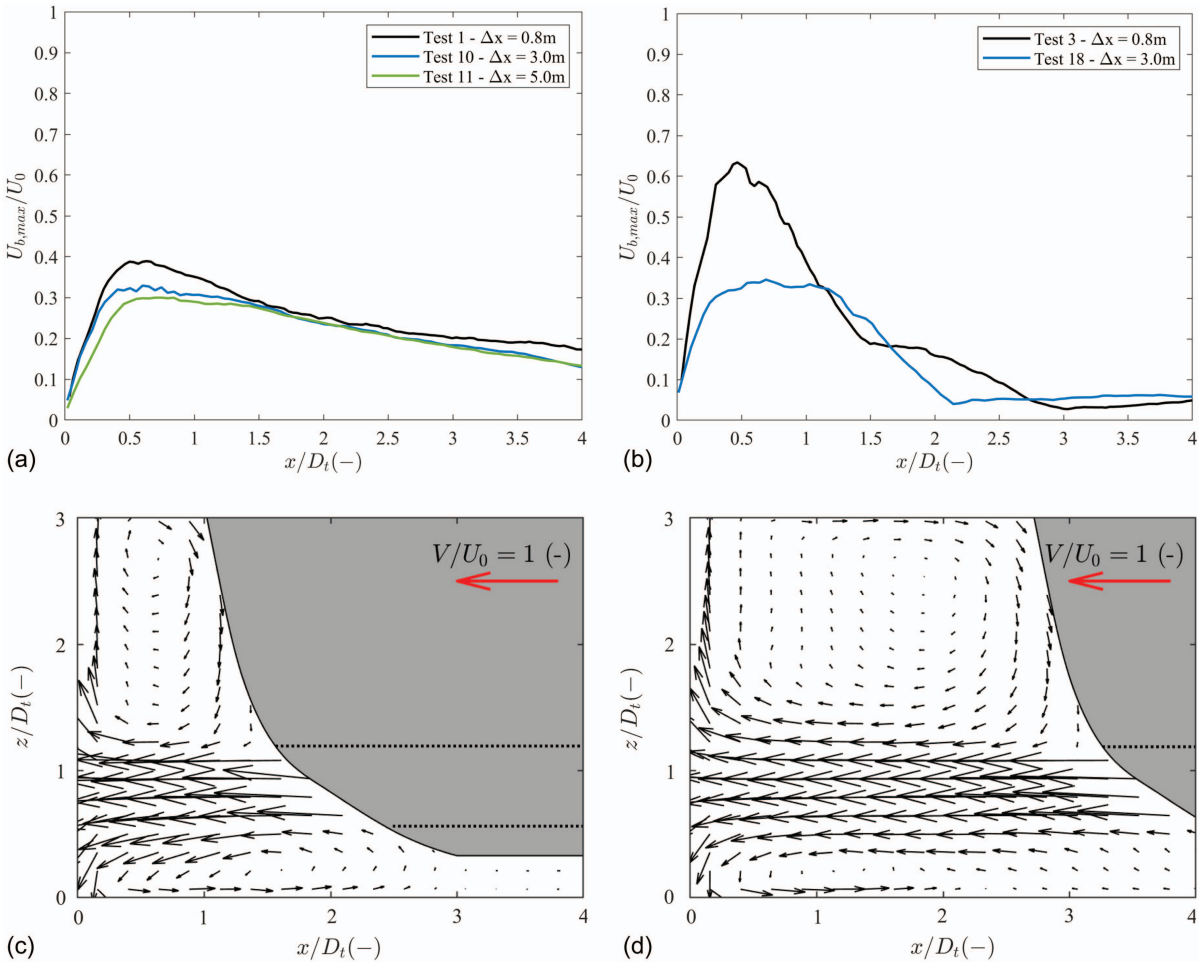

Fig. 9. (Color) Effect of variation of the quay wall clearance on the decay of the maximum time-averaged near-bed velocity: (a) UKC = 2.5 m; (b) UKC = 0.5 m; (c) test 3 ($\Delta x = 0.8$ m); and (d) test 18 ($\Delta x = 3.0$ m).

method, the near-bed velocity starts decreasing at the quay wall, potentially leading to an underestimation of the maximum near-bed velocity away from the wall, for multiple tested conditions [Figs. 10(a, c, and d)].

- The alternative method provides a fixed value for the maximum velocity up to $x/D_t < 1$. Beyond this point, the velocity decays following the trend provided by the BAW (2010) guidelines, with a slight adjustment. This formulation was intentionally set to be conservative for the range of tested parameters.
- Regarding the extent of the protection (away from the quay wall), the distance of about one ship width is typically used as reference (PIANC 2015). The results of this research show that there is margin to optimize this width since the measured velocity decay is overall sharper than anticipated by the guidelines.

Possible Scale Effects

As is common practice in engineering research, the results have been presented in prototype scale, even though the experiments were performed in a physical scale model. Regarding possible scale effects, the following note is added. The experimental setup is scaled using Froude scaling, ensuring the ratio of inertial over gravitational forces are kept similar between model and prototype scale. Froude scaling is applied in flows where these forces dominate, such as free-surface flows. However, in zones of high shear force, like the edges of the propeller jet and along hard interfaces such as the bed, viscous forces become more significant and Reynolds scaling should be applied. For Reynolds scaling, the Reynolds number should be similar for both prototype and model scales. In practice, it is not feasible to satisfy both Froude and Reynolds scaling simultaneously. Nevertheless, if the Reynolds number is kept sufficiently large in the scale model, such that the flow remains in the turbulent regime, scale effects may be considered limited. To fulfil this requirement, the flow Reynolds number should be greater than 3×10^3, according to Blaauw and van de Kaa (1978). Even though this criterion is satisfied during the tests, small deviations in flow velocity can occur due to the Reynolds dissimilarity, as momentum transfer is more significant at lower Reynolds numbers. Consequently, jet and near-bed velocities may be slightly underestimated when translating the results to prototype scale.

Conclusions

In this study, physical scale model tests have been performed measuring in high detail the near-bed flow velocities resulting from a confined bow thruster jet. Our investigation explored the effect of various parameters, focusing on the effect of the bed roughness, under-keel clearance, and quay wall clearance on the reflected jet near the bed. The main results show that increasing the bed roughness changes the flow patterns near the bed, resulting in an overall reduction of the

J. Hydraul. Eng., 2026, 152(1): 04025053

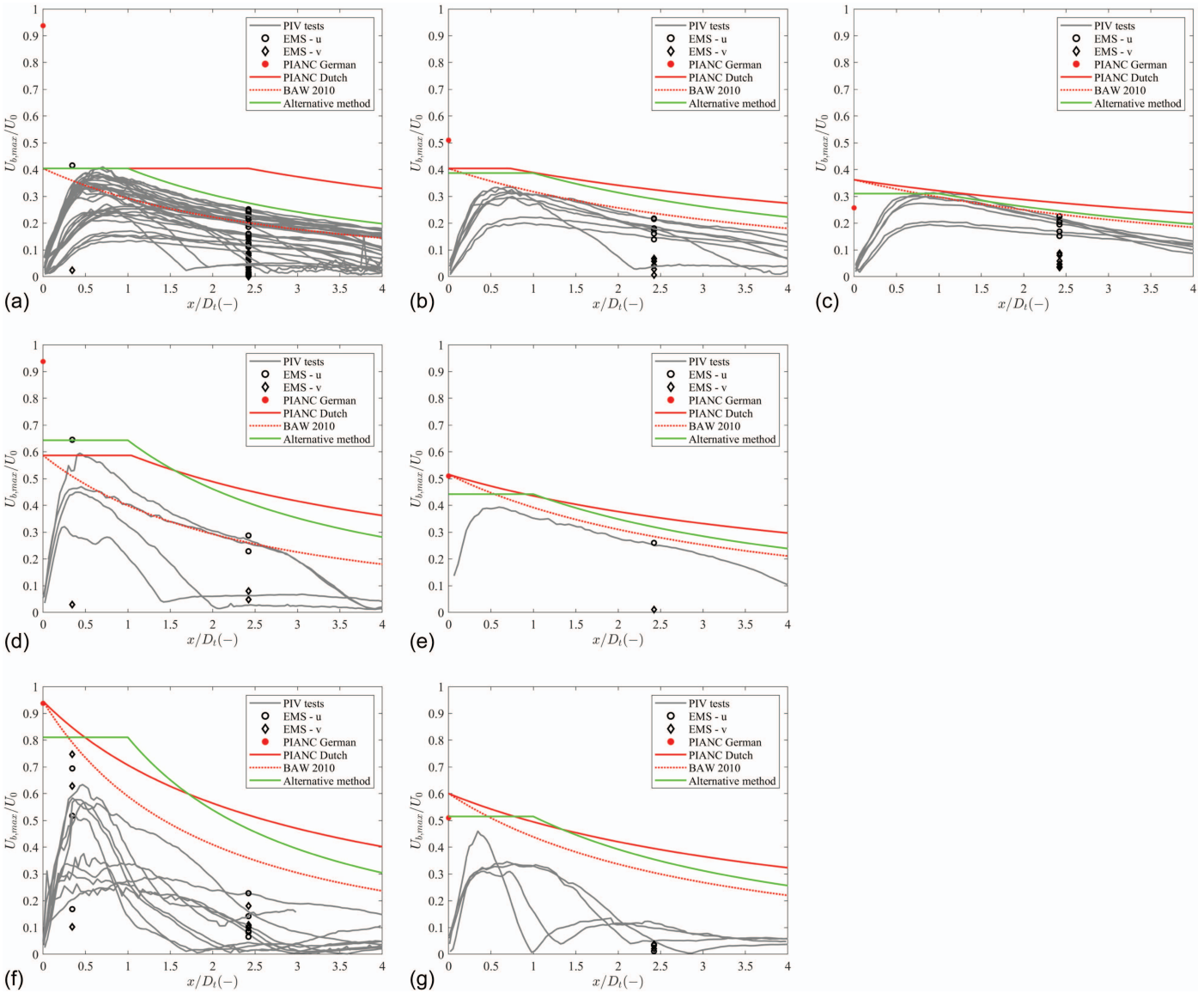

Fig. 10. (Color) Envelope of decay of the maximum time-averaged near-bed velocity measured with PIV (u-component), for all performed tests with varying UKC, quay wall clearance, bed roughness, Δy and propeller power. Comparison with the guidelines. For UKC = 2.5 m: (a) $\Delta x = 0.8$ m; (b) $\Delta x = 3.0$ m; and (c) $\Delta x = 5.0$ m; for UKC = 1.5 m: (d) $\Delta x = 0.8$ m; and (e) $\Delta x = 3.0$ m; and for UKC = 0.5 m: (f) $\Delta x = 0.8$ m; and (g) $\Delta x = 3.0$ m.

Table 6. Alternative formulation for the maximum near-bed velocity and decay of the maximum near-bed velocity for transverse thrusters

Source	Equation		Remark
Alternative formulation	$\frac{U_{b,\max}}{U_0} = \frac{D_t}{h_t}$	(17)	for $x/D_t < 1$, $\frac{L_{BT}}{h_t} < 1$
	$\frac{U_{b,\max}}{U_0} = 2.4\left(\frac{D_t}{L_{BT}+h_t}\right)$	(18)	for $x/D_t < 1$, $\frac{L_{BT}}{h_t} \geq 1$
	$\frac{U_{b,\max}(x)}{U_0} = \frac{D_t}{h_t}\left(\frac{L_{BT}+h_t}{L_{BT}+h_t+x-D_t}\right)^{1.4}$	(19)	for $x/D_t \geq 1$, $\frac{L_{BT}}{h_t} < 1$
	$\frac{U_{b,\max}(x)}{U_0} = 2.4D_t\frac{(L_{BT}+h_t)^{0.4}}{(L_{BT}+h_t+x-D_t)^{1.4}}$	(20)	for $x/D_t \geq 1$, $\frac{L_{BT}}{h_t} \geq 1$

near-bed flow velocities and a sharper velocity decay away from the quay wall. Reducing available clearances (both under-keel and quay wall) generally results in higher flow velocities near the bed due to less available space for the jet to dissipate. The flow velocities near the bed result from an interplay of effects, e.g., bed roughness, blockage by the vessel and available clearances.

The measurements were compared with existing methods in literature used to estimate near-bed velocities. The Dutch method in

J. Hydraul. Eng., 2026, 152(1): 04025053

PIANC (2015), or the BAW (2010) guidelines, are more suitable for estimating maximum near-bed velocities within their specified range of application and are slightly conservative in most cases, which is desirable. The decay trend of the near-bed flow velocity farther away from the quay wall is best captured by the BAW (2010) guidelines, however in some cases the measured velocities were higher than the predicted by these guidelines. The decay trend by the Dutch method, conversely, tend to be too conservative, i.e., the measured velocities decay faster than predicted by this method. Based on the performed measurements and existing guidelines, an alternative formulation is provided here for u-shaped vessels with bow thrusters channels. The results presented here show that the highest near-bed velocities occur in the vicinity of the wall, and the conservatism existing on the extension recommended by the guidelines can be reduced based on these results. A point of attention for bow thrusters with inlets underneath the vessel is the flow velocity just below the inlet. In this research a couple of PIV measurements were performed to capture the flow field underneath the inlet (not shown here), where the observed flow behavior is highly rotational and unstable (e.g., small moving tornado), which made it difficult to properly capture it with planar PIV. However, the velocities measured near the bed were considerably higher than the predicted by the guidelines in this region. For design purposes, it is therefore recommended to assess separately whether bed protection against thruster inlet flow velocities would be required at that location.

There are several aspects worth mentioning related to the limitations of this research. First, the findings and the proposed alternative approach are derived exclusively from experiments involving channel-type bow thrusters. Testing of other maneuvering systems and main propulsion units was outside the scope of this study. Furthermore, the study was based on a single size and geometry of bow thruster. To generalize the conclusions, further research is needed to validate the findings across a broader range of vessel shapes and thruster characteristics. Our study was designed to isolate the hydraulic effects of a bow thruster under controlled, still-water conditions, providing a clear baseline for understanding jet behavior. However, in practical applications, additional environmental factors—such as tidal currents, wave-induced motion, return flows from passing vessels, and groundwater inflow—can significantly influence the velocity field and associated risks. These influences may lead to underestimating the most vulnerable location if not properly accounted for. While our proposed approach captures the general decay behavior of the jet, it does not explicitly incorporate these external effects. While we propose an alternative formulation for estimating near-bed velocity and decay, we acknowledge the absence of a roughness parameter in our method. It can be desirable to include a roughness parameter since roughness has a very pronounced effect in reducing the near-bed flow velocities. For that, it is recommended considering a systematic variation of bed roughness together with the remaining relevant parameters in future research efforts. The effect of the quay-wall roughness has not been explicitly considered in this study. Real-world quay-walls may exhibit surface patterns or irregularities (e.g., sheet-pile walls), which could significantly influence the dissipation of ship induced jets. Additionally, this study focused on steady-state conditions only. However, intermittent thruster power during start-up situations may exert high loads on the bed. And finally, the definition of the efflux velocity remains important and the ambiguity in its formulation should be addressed.

In summary, detailed PIV measurements shed light on the flow patterns and velocities resulting from confined bow thruster jets. These insights can help engineers to optimize bed protection designs in the future by adopting the proposed alternative formulation.

Data Availability Statement

Some or all data, models, or code that support the findings of this study are available from the corresponding author upon reasonable request.

Acknowledgments

The authors would like to thank the CROW working group for making this research possible, in particular by the funding made available by Rijkswaterstaat, Port of Rotterdam Authority and the Dutch Government via the Top consortium for Knowledge and Innovation (TKI). The authors are grateful for the support and ingenuity provided by the Experimental Facility Support (EFS) department of Deltares.

Author Contributions

Helena I. S. Nogueira: Formal analysis; Investigation; Methodology; Supervision; Writing – original draft; Writing – review and editing. Christian van Nieuwenhuizen: Formal analysis; Investigation; Methodology; Writing – original draft; Writing – review and editing. Wout Bakker: Conceptualization; Formal analysis; Investigation; Methodology. Arne van der Hout: Funding acquisition; Investigation; Supervision; Writing – review and editing. Paolo Di Pietro: Conceptualization; Funding acquisition; Resources; Validation; Writing – review and editing. Charlotte van der Vorm: Funding acquisition; Resources.

Notation

The following symbols are used in this paper:

C_1, C_2 = dimensionless coefficients;
D = thruster channel (duct) diameter;
D_p = propeller diameter;
D_t = thruster diameter;
D_0 = diameter outflow opening;
f_n = percentage of maximum number of revolutions;
f_p = percentage of installed engine power, for propellers;
f_t = percentage of installed engine power, for thrusters;
h_t = vertical distance between axis thruster channel and bed;
K_t = thrust coefficient;
L_{BT} = quay wall clearance = horizontal distance between outflow opening and quay wall;
$n_{\max}$ = maximum number of revolutions;
P_D = maximum installed engine power;
$U_{b,\max}$ = maximum time-averaged near-bed velocity = local maximum velocity obtained from the velocity profile along the water column, near the bed;
U_{BT} = area averaged outflow velocity;
U_{wall} = maximum time-averaged velocity of the main jet, at the quay wall;
U_0 = efflux velocity = maximum outflow velocity;
u = velocity component in the x-direction;
v = velocity component in the y-direction;
w = velocity component in the z-direction;
x = horizontal direction away from the quay wall;
y = horizontal direction along the quay wall;
z = vertical direction away from the bed;
Δx = horizontal distance between port and quay wall;

Δy = horizontal distance between centerline bow thruster channel and PIV measurement plane;
ρ_w = density of water; and
ξ = energy loss coefficient.

References

Adrian, R., and J. Westerweel. 2011. *Particle image velocimetry*. New York: Cambridge University Press.

Albertson, M. L., Y. Day, R. Jensen, and H. Rouse. 1950. "Diffusion of submerged jets." *Trans. Am. Soc. Civ. Eng.* 115 (1): 639–664. https://doi.org/10.1061/TACEAT.0006302.

BAW (Bundesanstalt für Wasserbau). 2010. *BAW code of practice: Principles for the design of bank and bottom protection for Inland waterways*. Karlsruhe, Germany: BAW.

Blaauw, H. G., and E. J. van de Kaa. 1978. "Erosion of bottom and sloping banks caused by the screw race of manoeuvering ships." In *Proc., 7th Int. Harbour Congress*. Antwerp, Belgium: Section International Publications.

Blokland, T. 1996. *Bed protection loads by propeller jets* [In Dutch.] Rep. No. 61.00-r96.038. Rotterdam, Netherlands: Ingenieursbureau Havenwerken.

Brocca, G., A. J. van der Hout, T. Sattar, P. Di Pietro, H. Nogueira, C. van Nieuwenhuizen, and M. Vicari. 2024. "Innovative research on novelty environmentally friendly rock-filled mattress solution for scour prevention design in berthing structures." In *Proc., 35th PIANC World Congress*. Brussels, Belgium: Permanent International Association of Navigation Congresses.

Cantoni, I. 2020. "Bowthruster-induced flow on the bottom of a vertical quay wall." M.Sc. thesis, Faculty of Civil Engineering and Geosciences, Delft Univ. of Technology.

Coscarella, F., G. Curulli, N. Penna, and R. Gaudio. 2023. "Physically based formula for the maximum scour depth induced by a propeller jet." *Phys. Fluids* 35 (3): 035113. https://doi.org/10.1063/5.0140666.

Deltares. 2022. *Characterization of flows induced by propeller jets—Physical scale model test report*. Deltares Rep. No. 11206641-003-HYE-0001. Delft, Netherlands: Stichting Deltares.

Deltares. 2023. *RenoMac plus mattresses—PIV testing. PIV tests under propeller jet induced flows*. Deltares Rep. No. 11209082-000-HYE-0002. Delft, Netherlands: Stichting Deltares.

Fuehrer, M., K. Römisch, and G. Engelke. 1981. "Criteria for dimensioning the bottom and slope protections and for applying the new methods of protecting navigation canals." In *Proc., PIANC XXVth Congress*. Brussels, Belgium: Permanent International Association of Navigation Congresses.

Haafkes, T. 2021. "Numerical simulation of bow thruster induced near-bed flow next to quay wall." M.Sc. thesis, Faculty of Mechanical Engineering, Delft Univ. of Technology.

Hawkswood, M. G., G. M. Hawkswood, and M. Furborough. 2024. "Research and development in berth scour protection." In *Proc., 35th PIANC World Congress*. Brussels, Belgium: Permanent International Association of Navigation Congresses.

Hong, J., Y. Chiew, and N. Cheng. 2013. "Scour caused by a propeller jet." *J. Hydraul. Eng.* 139 (9): 1003–1012. https://doi.org/10.1061/(ASCE)HY.1943-7900.0000746.

Hong, J., Y. M. Chiew, S. Hsieh, N. Cheng, and P. Yeh. 2015. "Propeller jet-induced suspended-sediment concentration." *J. Hydraul. Eng.* 142 (4): 04015064. https://doi.org/10.1061/(ASCE)HY.1943-7900.0001103.

Meijer, D., and H. Verhey. 1993. *Flow velocities at the bank caused by bow thrusters* [In Dutch.] Rep. No. Q1657. Delft, Netherlands: Waterloopkundig Laboratorium.

Niewerth, S., F. Núñez-González, F. Llull, and S. Lempa. 2021. "A novel shear plate for direct measurements of bottom shear stress induced by a model ship propeller." In *Webinar on experimental methods and laboratory instrumentation in hydraulics*. Warsaw, Poland: Institute of Geophysics, Polish Academy of Sciences.

Núñez-González, F., J. A. Macías-Lezcano, and J. Aberle. 2022. "Boundary shear stress induced by a ship propeller wake over rough and smooth bed surfaces." In *Proc., River Flow 2022*. Boca Raton, FL: CRC Press.

PIANC (Permanent International Association of Navigation Congresses). 2015. *Guidelines for protecting berthing structures from scour caused by ships*. PIANC Rep. No. 180. Brussels, Belgium: PIANC.

RWS (Rijkswaterstaat). 2018. *Richtlijn ontwerp waterbow*. Utrecht, Netherlands: RWS.

Schmidt, E. 1998. "Ausbreitungsverhalten und erosionswirkung eines bug-propellerstrahls vor einer kaiwand." [In German.] Ph.D. thesis, Dept. of Hydraulic Engineering and Water Protection, Technical Univ. of Braunschweig.

Tukker, J. W. T. 2021. "Decay of bow thruster induced near-bed flow velocities at a vertical quay wall." M.Sc. thesis, Faculty of Civil Engineering and Geosciences, Delft Univ. of Technology.

van der Wart, L. 2022. "The potential benefits of standardisation of the design of bed protections at waiting places at ship locks in the Netherlands." M.Sc. thesis, Faculty of Civil Engineering and Geosciences, Delft Univ. of Technology. http://resolver.tudelft.nl/uuid:1d4161ac-7f4c-4e31-bab7-76d080985220.

van Nieuwenhuizen, C., A. J. van der Hout, H. Nogueira, W. Bakker, G. Brocca, and P. Di Pietro. 2024. "Physical modelling of propeller jet induced scour near quay walls." In *Proc., 9th Int. Conf. on Physical Modelling in Coastal Engineering (Coastlab24)*. Delft, Netherlands: TU Delft.

Verheij, H. 1983. "The stability of bottom and banks subjected to the velocities in the propeller jet behind ships." In *Proc., 8th Int. Harbour Congress*. Antwerp, Belgium: Section International Publications.

Wei, M., Y. Chiew, and N. Cheng. 2020. "Recent advances in understanding propeller jet flow and its impact on scour." *Phys. Fluids* 32 (10): 101303. https://doi.org/10.1063/5.0023266.

Wei, M. X., and Y. M. Chiew. 2017. "Influence of toe clearance on propeller scour around an open-type quay." *J. Hydraul. Eng.* 147 (7): 04017012. https://doi.org/10.1061/(ASCE)HY.1943-7900.0001303.

Wei, M. X., and Y. M. Chiew. 2018. "Characteristics of propeller jet flow within developing scour holes around an open quay." *J. Hydraul. Eng.* 144 (7): 04018040. https://doi.org/10.1061/(ASCE)HY.1943-7900.0001470.

Wei, M. X., and Y. M. Chiew. 2019. "Impingement of propeller jet on a vertical quay wall." *Ocean Eng.* 183 (73): 73–86. https://doi.org/10.1016/j.oceaneng.2019.04.071.

Wei, M. X., Y. M. Chiew, and D. Guan. 2018. "Turbulent flow field of propeller jet around an open-type quay." *J. Coastal Res.* 85 (May): 956–960. https://doi.org/10.2112/SI85-192.1.

Wei, M. X., Y. M. Chiew, and S. C. Hsieh. 2017. "Plane boundary effects on characteristics of propeller jets." *Exp. Fluids* 58 (10): 141. https://doi.org/10.1007/s00348-017-2425-8.

Westerweel, J., and F. Scarano. 2005. "Universal outlier detection of piv data." In Vol. 39 of *Experiments in fluids*, 1096–1100. New York: Springer.